

## Charge Transfer to the 2s State of Hydrogen from Close Collisions of $H^+$ with He and $Ar^{\dagger}$

D. H. Crandall\* and D. H. Jaecks

*Behlen Laboratory of Physics, University of Nebraska, Lincoln, Nebraska 68508*

(Received 18 March 1971)

Measurements of the electron-capture probability for close encounters in the reactions  $H^+ + He \rightarrow H(2s) + He^*$  and  $H^+ + Ar \rightarrow H(2s) + Ar^*$  are reported. The incident proton energies employed range from 3 to 20 keV. Measurements were made for particular impact parameters by selecting particular angles of scatter between 1 and 5 deg. The data show little angular dependence but exhibit structure as a function of collision time. For  $H^+ + He \rightarrow H(2s) + He^*$  this structure is similar to that observed previously by Everhart and co-workers for capture into all states of hydrogen for the reaction  $H^+ + He \rightarrow H + He^*$ , which is dominated by transfer to the 1s state of hydrogen. The present data are not in agreement with available coupled-state calculations for this process.

### I. INTRODUCTION

Measurements of charge-transfer cross sections and probabilities are of interest for testing the range of validity of various models used in calculations of atomic collision processes. One model based on the semiclassical impact-parameter approach has been used with some success in the theoretical calculations of some atomic collision processes.<sup>1</sup> For charge transfer, such calculations predict directly the probability of electron transfer to a particular state of the atom formed during an ion-atom collision at a particular classical impact parameter (scattering angle). Thus measurements of charge-transfer probabilities to particular atomic states, at particular scattering angles, provide a more direct comparison between theory and experiment than total-cross-sections measurements.

The measurements of Everhart and his colleagues<sup>2-4</sup> of the probability for forming atomic hydrogen (in all states) in close collisions, for reactions such as  $H^+ + H \rightarrow H + H^+$  and  $H^+ + He \rightarrow H + He^*$ , have provided important tests of theoretical calculations<sup>5-8</sup> (Refs. 5-8 are given as examples of the many coupled-state calculations relying on the impact-parameter approach). Usually the theoretically predicted probability for transfer to the 1s state of hydrogen is compared with the measurement of transfer probability to all states, since the total transfer is expected to be predominantly to the 1s state. However, measurements of the probability of transfer to particular atomic states give a more direct comparison with theoretical calculations and help to establish the relative contribution of particular states to the total charge-transfer process.

In this paper, measurements of the charge-transfer probability for formation of  $H(2s)$  from close collisions of  $H^+$  with He and Ar are presented. Measurements of the probability of transfer to all states of hydrogen for these collisions have also

been made, with good agreement between the present data and those of Ziemba, Lockwood, Morgan, and Everhart<sup>3</sup> and of Helbig and Everhart.<sup>4</sup>

Present measurements include the energy range 3-20 keV with scattering to angles between 1 and 5 deg. Data are presented for measurements at constant incident energy with varying scattering angle (impact parameter) and for varying incident energy at constant impact parameter. For classical trajectories the product of incident energy and laboratory scattering angle ( $\Theta T$ ) corresponds to a particular impact parameter  $\rho$ , according to Ref. 9:

$$\Theta T = -\rho \int_0^{\infty} \frac{\partial U}{\partial r} \frac{dr}{(r^2 - \rho^2)^{1/2}}, \quad (1)$$

where  $U$  is the interaction potential which is only a function of the internuclear separation  $r$ . The values of impact parameter given for the present data are obtained from the work of Dose,<sup>10</sup> where a screened potential allowing for a separate screening constant for each shell of electronic structure of the atom has been employed to evaluate this relationship.

The present results for the probability  $P_{2s}$  for forming  $H(2s)$  show some similarity to the results for  $P_0$ , the probability of forming hydrogen in all states, at least for the He case. An attempt is made to interpret these results in terms of the semiempirical equation presented by Helbig and Everhart<sup>4</sup> and discussed by Lichten.<sup>11,12</sup> For He, comparison is made between the present results and the coupled-state calculations of Sin Fai Lam<sup>8</sup> and the earlier constant-angle measurements by Dose and Meyer.<sup>13</sup>

### II. EXPERIMENT DESCRIPTION

#### A. Technique

The experimental arrangement is schematically

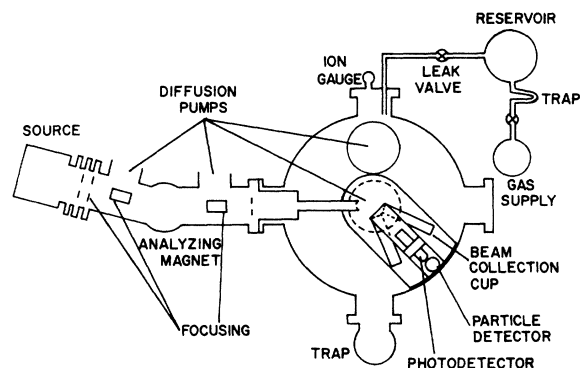


FIG. 1. General experimental arrangement (top view).

illustrated in Fig. 1. Protons were selected from the output of the duoplasmatron ion source by the analyzing magnet. The resulting beam of protons entered the scattering chamber through two circular apertures of 1.0-mm diam separated by 25.9 cm.

The interior of the scattering chamber (46 cm in diam) was filled with target gas at pressures of  $1 \times 10^{-3}$  Torr, or less. A differentially pumped, rotatable assembly housing the detectors received scattered particles from a portion of the length of target gas traversed by the proton beam. This assembly (Fig. 2) communicates with the interior of the scattering chamber only through the first of two apertures defining the scattered-particle acceptance geometry.

Figure 2 shows details of the detector arrangements as viewed from the side. Scattered particles enter the detector assembly from the left. A center slot is provided in the middle deflection plate to allow particles to pass through to the quenching capacitor and subsequently to strike the first stage of a bare-electron multiplier. When no voltage is applied to the deflection plates, both scattered fast protons and hydrogen atoms resulting from charge transfer are incident on the particle detector. With appropriate voltage applied to the deflection plates, the scattered protons are deflected, and only the fast hydrogen atoms reach the particle multiplier. Thus for any angle setting, the probability of charge transfer  $P_0$ , defined as the number of hydrogen atoms scattered divided by the total number of particles scattered, can be measured employing the deflection plates. Assuming equal detection efficiency of the bare multiplier for protons and for hydrogen atoms of the same velocity and holding the experimental parameters constant, the probability  $P_0$  is the direct ratio of the number of detected fast hydrogen atoms to the number of detected total particles.

If the scattered hydrogen atom is formed in the  $2s$  state by charge transfer, it will remain in that state through the detection region because of the

long lifetime of this state, 0.14 sec. However, the lifetime is reduced by application of an electric field which causes Stark mixing of the  $2s$  and  $2p$  states and subsequent decay to the ground state by emission of a Ly- $\alpha$  photon (1216 Å). The lifetime of the  $2s$  state in a field of 600 V/cm is reduced to about  $4.5 \times 10^{-9}$  sec.<sup>14</sup> In the present experiment the scattered particles pass through a quench capacitor which can be used to apply such electric fields. The hole in the front plate of the capacitor forms the second aperture defining the scattered-particle acceptance geometry.

A photodetector views the quenching region from above and counts a fraction of the total number of emitted Ly- $\alpha$  photons depending on photodetector efficiency, the solid angle from the quench region which the photodetector views, the fraction of the H( $2s$ ) atoms decaying within the quenching length viewed, and the angular distribution of the radiation.

The probability of transfer to the  $2s$  state  $P_{2s}$  was measured employing quenching as outlined. Assuming the radiation is isotropic, the probability can be written as

$$P_{2s} = \frac{N_{2s}/(\epsilon_p f)}{N_{tot}/\epsilon_m} = \frac{N_{2s}\epsilon_m}{N_{tot}\epsilon_p f}, \quad (2)$$

where  $N_{2s}$  is the number of  $2s$  photons detected,  $\epsilon_p$  is the photodetector efficiency times the solid angle it views,  $f$  is the fraction of the H( $2s$ ) atoms decaying in the quench length viewed,  $N_{tot}$  is the total number of hydrogen atoms plus protons detected by the bare multiplier, and  $\epsilon_m$  is the multiplier detection efficiency. The question of the angular distribution of the quenched radiation will be discussed in Sec. IID.  $N_{2s}$  was determined from the difference in photon counts with quench voltage applied and with the quench capacitor grounded. Determination of the apparatus quantities will be described in Sec. IIB.

Actual data collection was controlled by integration of the primary beam. One of the beam collection cups (depending on whether the assembly is at a positive or negative angle setting) collected the

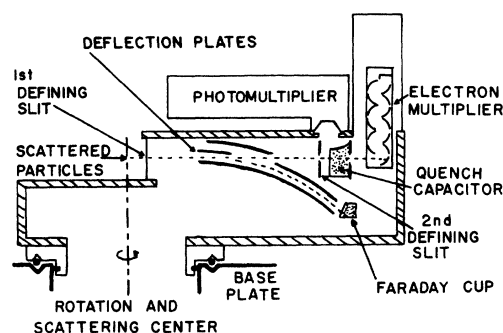


FIG. 2. Side view of rotatable assembly, showing detector arrangement.

primary beam. The total ion beam charge collected was stored by a current integrator. Data collections were repeated for quench voltage applied and for quench capacitor grounded, for deflection voltage applied and for deflection plates grounded, with target gas in the chamber and with the chamber evacuated. From these data,  $P_0$  and  $P_{2s}$  were determined for each angle and incident energy used.

Only for scattering angles less than  $2.5^\circ$  was appreciable background observed with the chamber evacuated. For these small angles the extremity of the primary beam could be reflected from the first slit defining the scattered particle acceptance geometry. Backgrounds, at small scattering angles, were 10–15% of the signals. These backgrounds were appropriately subtracted for the photon and scattered particle numbers used in determination of  $P_0$  and  $P_{2s}$ .

The differential cross sections for total scattering were also determined in the present experiment. This measurement required knowledge of the absolute target gas pressure, the beam collection efficiency, and the product of the solid angle of scattered particle acceptance times the length of the proton beam in the target gas viewed by the particle detector. The results for the total differential cross sections and the discussion of the related problems mentioned above are to be presented elsewhere.<sup>15</sup>

#### B. Apparatus Quantities

Target gas pressure was continuously monitored with a Bayard-Alpert ionization gauge which was calibrated and frequently checked against a McLeod gauge used as an absolute standard. Some care was taken with the McLeod gauge to reduce the known systematic errors.<sup>16</sup>

Care was also taken to assure that the data were not influenced by multiple collisions. Measurements of the number of scattered particles at small angles, and of emitted photons from the collision center, were made as a function of target gas pressure, at several energies. The intensity of these quantities is expected to vary linearly with pressure for single-collision conditions. All measurements were made with pressures well within the linear region.

The scattered-particle acceptance geometry is determined by two apertures (see Fig. 2). The first is a slit 0.513 mm wide by 31.8 mm long, where width is in the horizontal direction and length is in the vertical direction. This slit is 1.63 cm from the center of rotation of the detector assembly. This first slit is formed by the sides of two beam collection cups which are milled to knife edges. The second acceptance geometry aperture is a rectangular hole in the front plate of the quench capacitor. This aperture is 12.66 cm from the first slit. It is 1.01 mm wide by 3.73 mm long. The maximum

spread of the angle of scatter of particles entering this geometry is  $\pm \frac{1}{3}^\circ$ , determined by the widths of these apertures and the distance between them.

The width of the primary proton beam at the second defining slit of the rotatable detector assembly was measured by moving this slit across the beam. The beam was found to be sharply defined (with no gas in the chamber) and the total width at the second defining slit was observed to be 1.25 mm. Assuming a beam width of 1.00 mm entering the chamber (the size of the beam defining apertures), the corresponding angular divergence of the beam in the chamber was less than  $\pm 0.05^\circ$ .

The accuracy of the angle setting of the rotatable detector assembly has been taken to be  $\pm 0.05^\circ$ . The position was externally controlled by a hand crank and measured by a scale which divided turns of the crank into 100 parts. The reproducibility of an angle setting was found to be  $\pm 0.01$  turn or about  $\pm 0.03^\circ$ . In addition to reproducibility, the most serious limit to angular setting accuracy (at the small angles employed) is the alignment of the scattered-particle acceptance slits so that the first defining slit is accurately centered on the line between the scattering center and the second defining slit. This alignment and the general angular calibration were checked in several ways. Perhaps the most significant check were measurements of total scattering on either side of the zero angle position. Some small differences were observed at angles less than  $2^\circ$ , but were less than allowed for by the quoted angle setting accuracy of  $\pm 0.05^\circ$ .

Because of the construction geometry, all fast particles that enter the quenching region will be incident on the particle detector. Thus the particle acceptance geometry for the  $H(2s)$  atoms which emit  $Ly-\alpha$  photons is the same as for all other particles.

The bare-electron multiplier consists of 13 Cu-Be box structure dynodes. The scattered particles were incident on the first dynode (at ground potential) with the electron multiplier structures along a direction perpendicular to incoming particle motion. The electron multiplier was chosen over more recently developed continuous channel multipliers because of the relatively high particle counting rates employed (in excess of 50 kHz for periods of time exceeding several hours).

The efficiency of the multiplier for detection of fast hydrogen atoms was determined by measuring in coincidence the quench induced  $Ly-\alpha$  photons and the residual hydrogen atoms which strike the multiplier.<sup>17</sup> Each quench induced  $Ly-\alpha$  photon comes from one hydrogen atom which subsequently strikes the electron multiplier. Thus, every counted photon is associated with one hydrogen atom which will be detected with a certain efficiency. This efficiency can thus be obtained from the ratio of photon-particle coincidences to total photon counts. The effi-

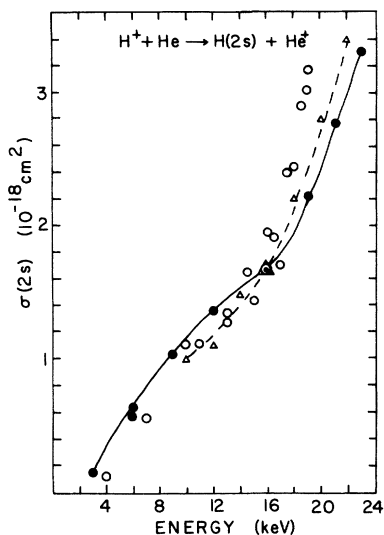


FIG. 3. Total cross section for transfer to H(2s) from protons incident on helium. ●-●-●, data of Jaecks *et al.*, Ref. 19; Δ-Δ-Δ, data of Andreev *et al.*, Ref. 20; ○ ○ ○, present data normalized to the others at 16 keV.

ciency values obtained by this method have been used for  $\epsilon_m$  in the reduction of the present data and were observed to vary almost linearly with incident ion energy from about 0.09 at 4 keV to 0.16 at 20 keV.

It has been assumed that the efficiency of the multiplier for detection of protons and hydrogen atoms of the same velocity is identical. This assumption has been used by other investigators (Ref. 3) and is supported by measurements of surface quantum efficiency for production of secondary electrons by atoms and ions of various charge states.<sup>18</sup> In the present case the efficiency of the multiplier was also checked by comparing measured and calculated differential cross sections for total scattering for H<sup>+</sup> on Ar. This check of efficiency agreed well with the coincidence measurements and showed no variation with the changing ratio of protons to hydrogen atoms in the scattered particles detected.<sup>17</sup>

The photodetector with LiF window is sensitive to radiation between 1050 and 1800 Å with a peak efficiency near the 1216-Å line to be detected.

The value of  $\epsilon_p$  in Eq. (2) was obtained by measuring the intensity of the quenched 2s radiation at 0° and identifying it with the total cross section for transfer to H(2s). For this measurement the electron multiplier was replaced by a Faraday cup for collection of the beam which passed through the acceptance geometry. This current was used as the normalizing beam current for determining the incident intensity in the data reduction. Data were taken at sufficiently low pressures so that no decrease in measured current was observable as gas

was introduced into the collision chamber.

In order to identify the measurements at 0° with the total cross section for charge transfer to H(2s), it is necessary to determine the fraction of the H(2s) atoms which are scattered out of the acceptance geometry during the charge-changing collisions. By examining the quench induced photon yield at small scattering angles near 0°, with and without target gas in the scattering chamber, it was established that less than 7% of the H(2s) atoms formed at 4 keV, H<sup>+</sup>-Ar collisions, were scattered out of the acceptance geometry. Since the differential cross section has a  $1/T^2$  dependence, an even smaller fraction of the H(2s) atoms formed will be lost at higher energies.

The present results for the total cross section for transfer to H(2s) for H<sup>+</sup> + He → H(2s) + He<sup>+</sup>, normalized to the previous results of Jaecks, Van Zyl, and Geballe<sup>19</sup> and of Andreev, Ankudinov, and Bobashev<sup>20</sup> at 16 keV, are shown in Fig. 3. This normalization does not include correction for H(2s) lost by scattering since from the above arguments it should be small at 16 keV. This normalization was used to determine a value of  $\epsilon_p$ . Using this value, the cross section for total transfer to H(2s) in proton-argon collisions was measured. The results agreed with those of other investigators<sup>19-21</sup> within quoted uncertainties.

The value of  $\epsilon_p$  was also estimated using the manufacturer's quoted efficiency for the photodetector, with measurements for the efficiency of transmission of pulses by the electronics and calculated solid angles. This estimate of  $\epsilon_p$  was within 10% of the result obtained by the normalization process. The value of  $\epsilon_p$  used in the reduction of the present data is the one determined by normalization to previous work. Errors in determining  $\epsilon_p$  due to a nonisotropic distribution of the quenched Ly-α radiation will be discussed in Sec. II D.

Since the photodetector views a finite length of the quenching region it is possible that some fraction  $f$  of the H(2s) atoms may pass beyond the view of the photodetector before decay and emission of a photon. This can happen even though the quenching field is made sufficiently strong that saturation of the observed Ly-α signal is obtained (Fig. 4). For sufficiently fast atoms, some may still pass beyond the length viewed. This fraction [ $f$  in the definition of  $P_{2s}$  in Eq. (2)] will change with changing velocity of the atom in the quenching region.

An estimate for the change in the fraction  $f$  with changing energy was calculated. In order to estimate the lifetime, it was necessary to determine the field along the axis of the quenching capacitor. The capacitor consists of a grounded front plate with a shallow closed cylinder forming the other electrode. The construction was to help shield the quenching region from stray electrons and photons.

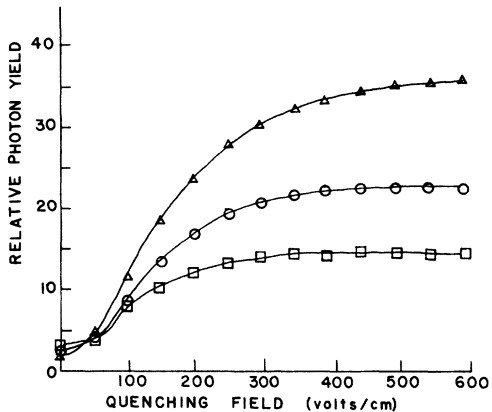


FIG. 4. Photon yield as a function of applied quenching field. Incident proton energies are: 5 keV, □; 10 keV, ○; 15 keV, △.

The potential at points inside the capacitor was calculated employing a numerical technique. For  $-905$  V applied to the closed cylinder end, the field along the axis of the capacitor was found to vary from 660 to 250 V/cm, with the region directly viewed by the photodetector averaging about 550 V/cm. The lifetime of the 2s state  $\tau_{2s}$  was determined from the expression given by Bethe and Salpeter<sup>22</sup>

$$\tau_{2s} = \tau_{2p} \left( 1 + \frac{M^2}{[1 - (1 + M^2)^{1/2}]^2} \right), \quad (3)$$

where  $\tau_{2p}$  is the lifetime of the 2p state of hydrogen and  $M$  is the field interaction,  $M = 2\sqrt{3}Eea_0/L$ , with  $L$  the Lamb shift,  $a_0$  the Bohr radius,  $e$  the electronic charge, and  $E$  the field strength.

The fraction of H(2s) atoms decaying in the length viewed by the photodetector was then calculated employing the expression

$$f = \frac{\int_0^l e^{-x/v\tau_{2s}} dx}{\int_0^\infty e^{-x/v\tau_{2s}} dx}, \quad (4)$$

where the time in the field has been expressed in terms of the velocity of the atom. The results indicated that, at 1 keV energy, 99% of the H(2s) atoms decay in the length of quench region viewed, but at 20 keV only 69% decay within this length. The fraction  $f$  was calculated for each energy used and employed in the determination of  $P_{2s}$  as indicated in the definition (2).

It should be noted that our previously reported preliminary results<sup>23</sup> did not include this fraction  $f$  in the reduction of  $P_{2s}$ . Also, the preliminary results were obtained by using calculated Rutherford cross sections for the total scattering rather than the experimentally determined total scattering cross sections.<sup>15</sup>

#### C. Sources of Experimental Error

In addition to possible error in the normalization

process several other sources could introduce error in the measurement of the quench induced Ly- $\alpha$  photon intensity. They include (i) cascade from higher states to the 2s state, (ii) quenching of H(2s) metastables before the region viewed by extension of the electric field through the entrance hole in the front plate of the capacitor, and (iii) polarization of the quench induced radiation.

The increase in the H(2s) population due to cascade from higher states can be estimated using the measurements of total cross sections for production of H(3p) and H(4p) due to collisions of H<sup>+</sup> with He and Ar reported by Hughes, Stigers, Doughty, and Stokes.<sup>24</sup> The H(3p) cross section is given by this work, but the H(4p) cross section was estimated from the measurement of H(4s). With these cross sections and the branching ratios for the decay of these states,<sup>22</sup> the cascade contribution from these states can be estimated. Cascade from higher states decreases rapidly since the total cross sections for transfer decrease roughly as  $n^{-3}$  according to Hughes *et al.* The estimated increase in H(2s) population for cascade from all higher states is 4–5% for both He and Ar targets throughout the energy region investigated.

It should be pointed out that the earlier measurements of total H(2s) cross sections<sup>19,20</sup> used for the normalization, should contain less cascade contribution than the present data because of the placement of the quenching field in the collision region.

Some of the H(2s) photons may be quenched before entering the quenching region viewed by the photodetector if the quenching field extends through the hole in the front plate of the capacitor. This pre-quenching loss was estimated to be that due to a field of one-half the maximum value just inside the quench capacitor extending a length of one-half the width of the aperture. This estimate of the loss of H(2s) atoms due to prequenching varies from 7% at 4 keV to 3% at 20 keV.

#### D. Polarization of Quench Induced Radiation

The polarization of quench induced radiation presents a greater problem. The previous investigators<sup>19–21</sup> assumed the radiation induced by coupling the 2s and 2p states was isotropic. This assumption was based on the relative magnitudes of the fine-structure splitting between  $^2P_{1/2}$  and  $^2P_{3/2}$ , and the Lamb shift between  $^2P_{1/2}$  and  $^2S_{1/2}$  states. Since the Lamb shift is only 10% of the fine-structure splitting, it was assumed that Stark mixing would couple the  $^2S_{1/2}$  state predominantly to the  $^2P_{1/2}$  state so that the resulting radiation would be isotropic.

In 1968, Fite, Kauppila, and Ott<sup>25</sup> reported measurements of the polarization of radiation induced by weak-field quenching of H(2s) atoms excited by electron impact. They observed the polarization  $P$  for a quenching field of 15 V/cm to be

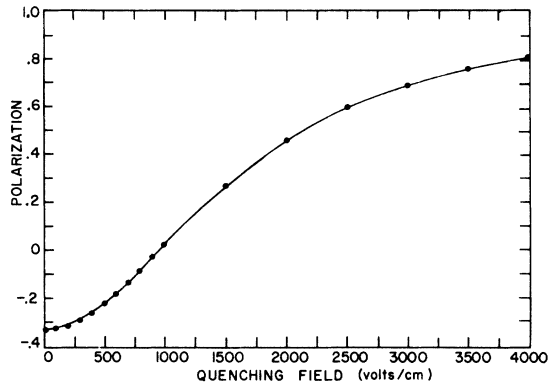


FIG. 5. Calculated polarization of quench induced Ly- $\alpha$  radiation as a function of quenching field.

$$P = \frac{I_{\parallel} - I_{\perp}}{I_{\parallel} + I_{\perp}} \Big|_{90^{\circ}} = -0.30 \pm 0.02, \quad (5)$$

where  $I_{\parallel}$  is the intensity of radiation along the field and  $I_{\perp}$  is the intensity of the radiation perpendicular to the field, observed at  $90^{\circ}$  to the field. Ott, Kauppila, and Fite<sup>26</sup> calculated the polarization employing time-independent perturbation theory to find the relative mixture of  ${}^2P_{1/2}$  and  ${}^2P_{3/2}$  states. The polarization predicted by this calculation was  $-0.329$ , in reasonable agreement with their experiment.

In the presence of stronger fields, the polarization may be modified from the value given above. Sellin, Biggerstaff, and Griffin have calculated the polarization of the quenched 2s radiation as a function of electric field strength for the case where the atom enters the quench field adiabatically.<sup>27</sup>

However if the atom enters the electric field region in a nonadiabatic manner, it is not clear that the results of Sellin, Biggerstaff, and Griffin will hold. Following the suggestions of Macek,<sup>28</sup> a calculation has been performed to determine the polarization of radiation induced by the quench fields of various strengths under conditions where the H(2s) atom enters the field in a time  $\Delta t$  such that  $\Delta E \Delta t \leq \hbar$ , where  $\Delta E$  is the fine-structure splitting of the 2p state.<sup>29</sup>

The calculation performed has ignored the widths of the P states and the hyperfine structure. The wave function  $\psi$  for the atom in the quenching field can be expanded in terms of the unperturbed atom wave functions for the  ${}^2S_{1/2}$ ,  ${}^2P_{1/2}$ , and  ${}^2P_{3/2}$  states with  $n=2$ . Using the standard transformation theory<sup>30</sup> and the assumption that initially the atom is in the  $n=2$ ,  ${}^2S_{1/2}$  state, the wave function  $\psi$  was constructed. The radiation from the atom represented by  $\psi$  to the ground state  $\phi_0$  is given by

$$I_{\text{tot}} \propto \int d\Omega \int_0^{\infty} \sum_{q=-1}^1 (\phi_0 | X_q | \psi)^* (\phi_0 | X_q | \psi) dt, \quad (6)$$

where  $(\phi_0 | X_q | \psi)$  is the usual dipole matrix element for a radiative transition and  $X_q$  is the component of  $X$  along polarization direction  $q$  where  $q = +1, 0, -1$ . The components of the radiation,  $I_{\parallel}$  along the field (associated with  $q=0$ ), and  $I_{\perp}$  perpendicular to the field (associated with  $q = +1$  and  $-1$ ) were determined from (6) for various field strengths ( $\psi$  is dependent on the field strength). The results for the polarization (5) as a function of field strength are shown in Fig. 5. For low fields, this calculation is in agreement with those of Ott *et al.*<sup>26</sup> and Sellin *et al.*<sup>27</sup>

The intensity observed at some angle relative to the quenching field can be written as

$$I(\theta) = \frac{I_{\text{tot}}}{4\pi} \frac{3(1 - P \cos^2\theta)}{3 - P} \quad (7)$$

employing the polarization as defined in Ref. 31. For the present experimental situation, with the detector at  $90^{\circ}$  to a field of about 600 V/cm, the predicted polarization is  $-0.20$  for the present calculation with the H(2s) atom entering the field suddenly. According to Sellin *et al.* the polarization is  $-0.55$  if the atom enters adiabatically.<sup>27</sup> These correspond to intensities,  $I(90^{\circ})$ , of  $I_{\text{tot}}(0.94)/4\pi$  for the sudden case and  $I_{\text{tot}}(0.85)/4\pi$  for the adiabatic case. Thus the radiation may be 6–14% lower than for an isotropic distribution.

An error due to the polarization may exist in all the measurements of the cross section for production of H(2s) that rely on electrostatic quenching. The experiment of Andreev *et al.*<sup>20</sup> employed a field of 600 V/cm with the photodetector at  $90^{\circ}$  to the field direction. This experiment, in which the H(2s) atoms were formed in the electric field, is thus a clear case where the sudden approximation is valid. The sudden approximation outlined above does not apply, however, since the polarization of the 2s and 2p state radiation must be determined simultaneously, since radiation from both is observed. The experiment of Jaecks *et al.*<sup>19</sup> quenched the 2s state in the region where it was formed, in a manner similar to that of Andreev *et al.*<sup>20</sup>; however, the quench field was made to reverse direction several times within the region viewed by the photodetector. For the experiment of Bayfield<sup>21</sup> the quenching field strength and direction have not been specified.

Because of the uncertainty in the cited published results used for normalization, no attempt was made to correct our present data for polarization effects. The agreement among previous investigators<sup>19–21</sup> is generally within their quoted errors of 20–40%. Because of this and the consistency between our normalization and the use of the manufacturer's quoted efficiency for determining  $\epsilon_p$  for our photodetector, it is expected that errors due to polarization may not be much greater than the 6–14% calculated for the present case. Neverthe-

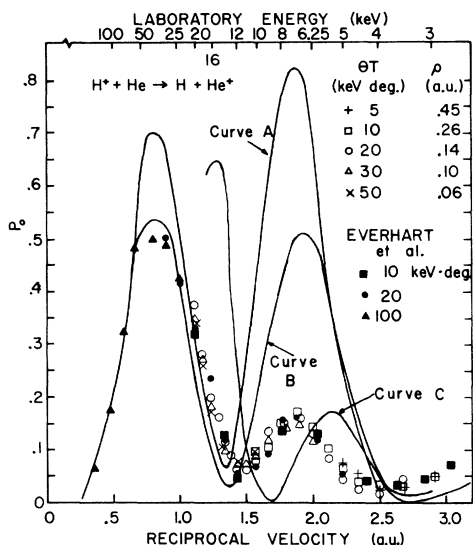


FIG. 6. Probability of transfer to all states of hydrogen from protons on helium. +, □, ○, △, ×, present data; ■, ●, ▲, data of Helbig and Everhart, Ref. 4. Curve A: calculation of Sin Fai Lam (Ref. 8) for transfer to H(1s, 2s, 2p) at  $\theta T = 20$  keV deg. Curve B: calculations of Green (Ref. 32) for transfer to H(1s) at  $\theta T = 20$  keV deg. Curve C: calculations of Colegrave and Stephens (Ref. 33) for transfer to H(1s) at  $3^\circ$ .

less, polarization of quench induced radiation is a continuing problem. The information presented here may be useful to future investigators employing electrostatic quenching of H(2s).

Considering the quoted errors of the measurements used for normalization and the sources of error mentioned above, the accuracy of our normalization should be  $\pm 50\%$ . This seemingly poor accuracy is sufficient for drawing specific conclusions about the data and related theories, for, as we shall see in Sec. III A, theory and experiment differ by factors of 10.

### III. RESULTS AND DISCUSSION

#### A. Protons on Helium

The present measurements together with measurements of Helbig and Everhart<sup>4</sup> and several calculations of  $P_0$  for  $H^+ + He \rightarrow H + He^+$  are shown in Fig. 6. The calculations of Sin Fai Lam<sup>8</sup> and Green, Stanley, and You-Chien Chian<sup>32</sup> are coupled-state calculations employing expansion of the wave function for the system in terms of eigenfunctions of the individual atoms, the former employing an expansion involving five atomic states and the latter employing two atomic states. The calculation of Colegrave and Stephens<sup>33</sup> is a perturbed state calculation with a two-state expansion of the system wave function in eigenfunctions of the quasimolecule. The damped oscillating behavior which is

regular in the collision time (reciprocal velocity) has been termed "quasiresonant" and is discussed by Lichten.<sup>11,12</sup>

The term "resonance" stems from the quantum-mechanical description of the  $H_2^+$  molecule.<sup>34</sup> It is the interference between symmetric and antisymmetric states of the quasimolecule of  $H_2^+$  formed during the collision  $H^+ + H$  which gives rise to the oscillation of charge-transfer probability observed by Lockwood and Everhart.<sup>2</sup> During the collision the oscillation of electronic charge between the lowest symmetric and antisymmetric states takes place. As the collision time decreases, the electron is left first with one nucleus, and then, when the collision is shorter by one-half the charge oscillation period, it is left with the other nucleus.

Lichten gives criteria for this same interference to arise in nonsymmetric collisions, such as  $H^+ + He$  where the resonance will be damped because the separated atom configurations have different energies after charge transfer. The criteria are that the collision be sufficiently sudden so that transitions take place in the quasimolecule in spite of the energy difference, and that the energy levels of the interfering states be widely separated during the collision so that many oscillations of the electron charge will occur during the collision time. The two conditions for quasiresonance are then (in a.u.)

$$|E_2(0) - E_1(0)| \gg 1/\tau \gg |E_2(\infty) - E_1(\infty)|, \quad (8)$$

where  $\tau$  is the collision time and the quantities in parentheses are the internuclear separations.

From Fig. 7, a correlation diagram for  $HHe^+$  from the work of Michels,<sup>35</sup> it can be seen that for  $H^+ + He \rightarrow H(1s) + He^+$  the conditions (8) are  $2.2 \text{ a.u.} \gg 1/\tau \gg 0.40 \text{ a.u.}$  Approximate values for the range of  $1/\tau$  in the present experiment are  $0.5\text{--}1.2 \text{ a.u.}$  so that quasiresonant oscillation of  $P_0$  is expected.

Lockwood and Everhart<sup>2</sup> and Helbig and Everhart<sup>4</sup>

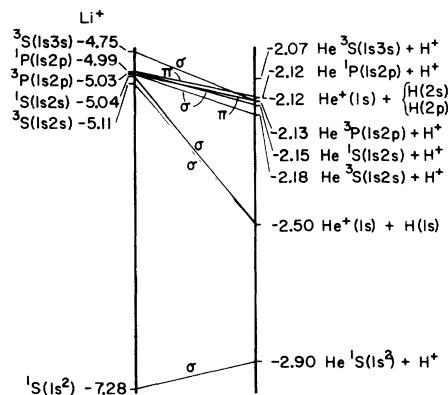


FIG. 7. Correlation diagram for states of  $(HeH)^+$ , from Michels, Ref. 35. Energies are in a.u.

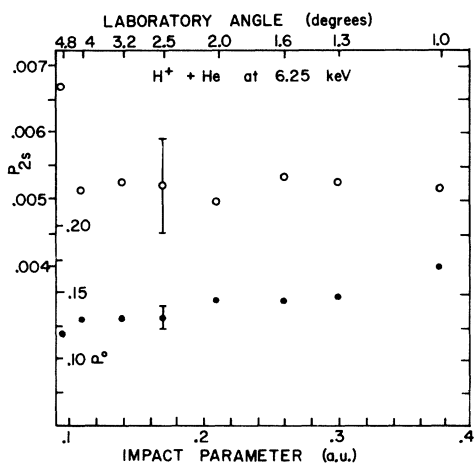


FIG. 8. Probability of transfer to H(2s) and to all states of hydrogen ( $P_0$ ) for protons on helium at 6.25 keV, as a function of impact parameter.

represented the oscillation of charge-transfer probability  $P_0$  for  $H^+ + H$  and  $H^+ + He$  by an empirical formula of the form

$$P_0 = A \sin^2(\langle Ea \rangle / 2v - B) \quad (9)$$

where  $E$  is the energy separation of the states,  $a$  is the distance over which the collision takes place, and  $B$  is the empirical value of the phase of the oscillations. The quantity  $\langle Ea \rangle$  is determined from the data. The period of oscillation of the electron between the states of the quasimolecule is

$$T = \hbar/E = a/v_n - a/v_{n+2},$$

where the  $n$  denotes any peak or valley of the observed oscillation in charge transfer. Expression

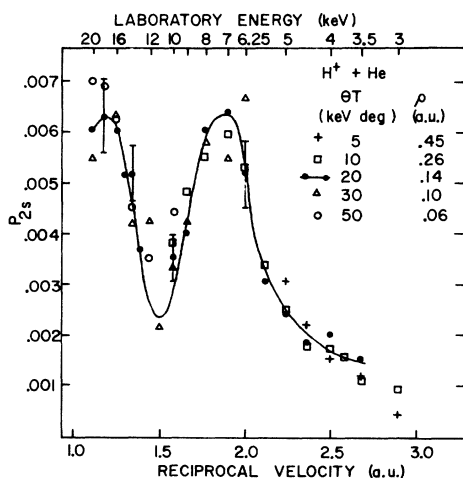


FIG. 9. Probability of transfer to H(2s) from protons on helium at several impact parameters, as a function of reciprocal velocity.

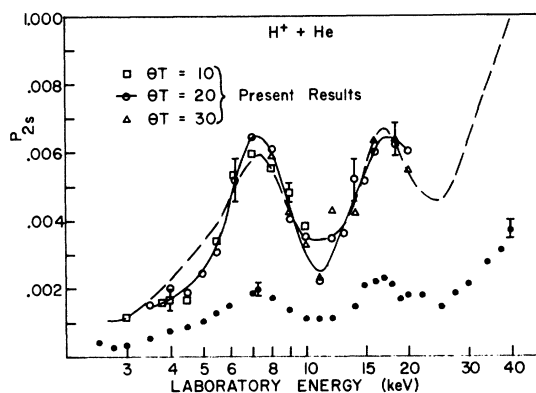


FIG. 10. Comparison of present measurement of  $P_{2s}$  with that of Dose and Meyer (Ref. 13).  $\Delta$ ,  $\square$ ,  $\circ$ , present data;  $\bullet$ , data of Dose and Meyer at  $2.2^\circ$ ; ---, data of Dose and Meyer multiplied by 3.

(9) has been found to fit the data for  $P_0$  from  $H^+ + H$  and  $H^+ + He$  with  $B$  nearly  $\frac{1}{4}\pi$  in both cases.

As indicated in Fig. 6, quantitative coupled-state calculations predict oscillation of  $P_0$  with the correct phase, but incorrect amplitude.

For the reaction  $H^+ + He \rightarrow H(2s) + He^+$ , it is not obvious from the qualitative discussion above that quasidegenerate (and hence oscillation) of  $P_{2s}$  should be expected. The quasidegenerate conditions (8) are still approximately satisfied,  $2.2 \gg 1/\tau > 0.73$  with  $1/\tau$  between 0.5 and 1.2 a.u. However, the population amplitudes of several nearly degenerate states, near the one which tends to  $H(2s) + He^+$ , rule out a simple two-state interpretation.

The present experimental results indicate that the quasidegenerate oscillation of  $P_{2s}$  remains, at least in part. Figure 8 indicates that  $P_0$  and  $P_{2s}$  do not exhibit large structure at a constant impact energy (collision time) for the range of impact parameters tested. Figure 9 illustrates that at least two distinct maxima occur in  $P_{2s}$  as a function of collision time for the values of impact parameters which cover the entire range.

Figure 10 shows comparison of the earlier measurements by Dose and Meyer<sup>13</sup> at a fixed scattering angle of  $2.2^\circ$ . Dose and Meyer did not have any convenient way to normalize their results. The experimental results were normalized to the Born approximation for  $H^+ + He \rightarrow H(2s) + He^+$  at 40 keV, which is of doubtful validity. Except for a difference of a factor of 3 in absolute value, the agreement is quite good. This is expected since the previous two figures demonstrate that the primary dependence of  $P_{2s}$  is on collision time and not impact parameter over the range measured. The results of Dose and Meyer indicate a third peak in  $P_{2s}$  is likely at some energy above 60 keV.

Application of the empirical formula (9) to the



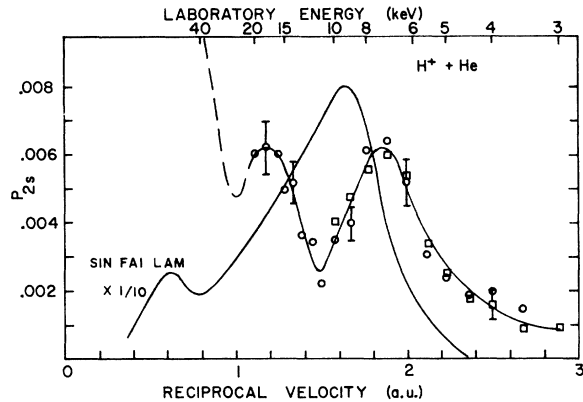


FIG. 11. Comparison of measurement of  $P_{2s}$  with prediction of the coupled state calculation by Sin Fai Lam (Ref. 8).  $\circ$ , present data  $\Theta T = 20$  keV deg;  $\square$  present data  $\Theta T = 10$  keV deg. Solid Curve: coupled-state calculation of Sin Fai Lam for  $\Theta T = 20$  keV deg times 1/10.

present data for  $P_{2s}$  requires estimating  $\langle Ea \rangle$  with the two peaks available. Nevertheless, estimating  $\langle Ea \rangle$  to be 9 a.u. and using Everhart's value of  $B = \frac{1}{4}\pi$ , we find that  $\sin^2(\langle Ea \rangle / 2v - \frac{1}{4}\pi)$  is a minimum at 10 and 30 keV and is a maximum at 6.3, 16, and 85 keV. This is in good agreement with the observed behavior and predicts the third maximum at 85 keV.

In Fig. 11 the present data are compared with the predictions of the four-state coupled-state calculations of Sin Fai Lam<sup>8</sup> for  $H^+ + He$ . For  $P_{2s}$ , it is seen that the quantitative theory differs by a factor of 10 from present results and the predicted oscillations are not in phase with those observed. In a previous paper,<sup>36</sup> the failure of the coupled-state calculations was suggested to be partly due to failure

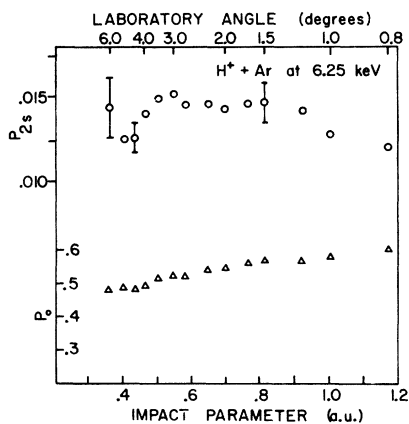


FIG. 12. Charge-transfer probabilities for  $H^+ + Ar$  at fixed impact energy 6.25 keV as a function of scattering angle.  $\circ$ , probability of transfer to  $H(2s)$ ;  $\Delta$  probability of transfer to all states of hydrogen (present results).

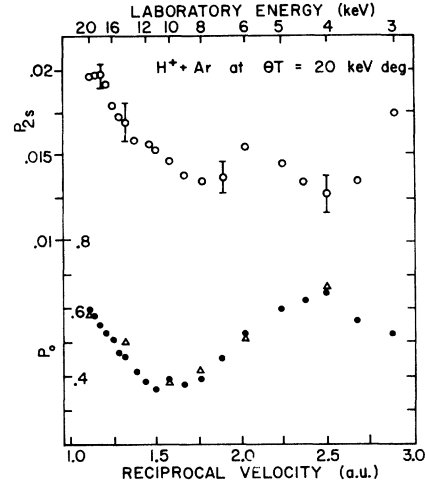


FIG. 13. Charge-transfer probabilities for  $H^+ + Ar$  at fixed impact parameter ( $\Theta T = 20$  keV deg;  $\rho = 0.53$  a.u.) as a function of inverse velocity.  $\circ$ , probability of transfer to  $H(2s)$ ;  $\bullet$  present data, probability of transfer to all states of hydrogen;  $\Delta$ , data of Everhart *et al.* (Ref. 3), probability of transfer to all states of hydrogen.

to include the excitation channels  $H^+ + He \rightarrow H^+ + He(2^1S, \text{ and } 2^1P)$  which are nearly degenerate with the charge transfer channels of interest  $H^+ + He \rightarrow H(2p, 2s) + He^+$ .

The error bars shown for  $P_{2s}$  in all of the figures represent the standard deviations of five or more trials of those particular data, and thus represent reproducibility. Nearly all of the  $P_{2s}$  data are averages of at least four measurements. The absolute error for  $P_{2s}$  is estimated at  $\pm 50\%$ , as stated previously. Values of  $P_0$  are accurate to  $\pm 10\%$ .

It might be noted that the contribution of  $P_{2s}$  to  $P_0$  is small. Measurements<sup>37</sup> of  $P_{2p}$  indicate that the  $2s$  and  $2p$  contributions to the charge transfer are only about 1–2%. Higher states are expected to contribute even less. Thus  $P_0$  is dominated by transfer to  $H(1s)$  for the  $H^+ - He$  system.

#### B. Protons on Argon

For protons on argon, no quantitative calculations for  $P_0$  or  $P_{2s}$  are available. However,  $P_0$  exhibits quiresonant behavior.

Figure 12 indicates that at a constant collision time corresponding to an incident energy of 6.25 keV,  $P_0$  is nearly constant where  $P_{2s}$  may contain some small structure. Figure 13 shows regular oscillation of  $P_0$  with changing collision time as expected for quiresonant behavior.  $P_{2s}$  for  $\Theta T = 20$  keV deg exhibits oscillatory structure of a higher frequency than  $P_0$ ; however, the data are not precise enough for any meaningful analysis.

Figure 14 shows the lowest levels of the united and separated limits for  $(H + Ar)^+$ .<sup>38</sup> No attempt at

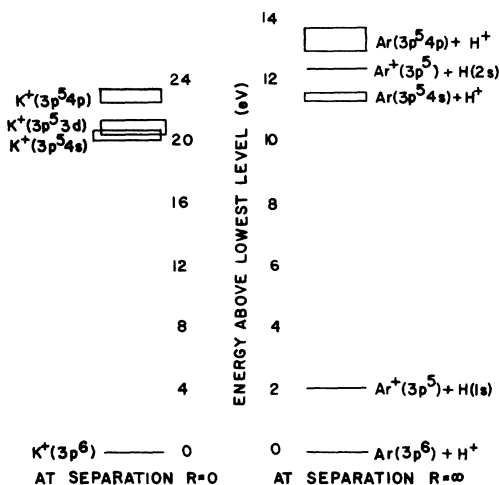


FIG. 14. Lowest energy levels of  $(Ar+H)^+$  and  $K^+$ .

correlation of energy levels has been made. However, charge transfer to  $H(1s)$  is expected to take

place between states of the quasimolecule involving the lowest level and one of the higher levels indicated of the united atom and involving the two lowest levels of the separated atom limit. Using the energy differences from Fig. 14, it can be seen that the quaresonance conditions (8) are reasonably well satisfied for  $P_0$ .

The uncertainties in  $P_{2s}$  and  $P_0$  for protons on argon are the same as for helium. However, the larger cross section allowed easier differential measurements for the argon case.

#### ACKNOWLEDGMENTS

The writers are indebted to Dr. J. Macek for continuing interest in this work and for his stimulating discussions and suggestions. The technical assistance of Peter Martin and Robert Dubois is appreciated. Dr. R. H. McKnight shared the apparatus during this project while conducting the experiments reported in the following paper. His contributions to the present work were many and varied.

- <sup>†</sup>Work supported by the National Science Foundation.  
<sup>\*</sup>Present address: JILA, Boulder, Colorado.  
<sup>1</sup>D. R. Bates and R. McCarroll, *Advan. Phys.* **11**, 39 (1962).  
<sup>2</sup>G. J. Lockwood and E. Everhart, *Phys. Rev.* **125**, 567 (1962); also H. F. Helbig and E. Everhart, *ibid.* **140**, A715 (1965).  
<sup>3</sup>F. P. Ziemba, G. J. Lockwood, G. H. Morgan, E. Everhart, *Phys. Rev.* **118**, 1552 (1960).  
<sup>4</sup>H. F. Helbig and E. Everhart, *Phys. Rev.* **136**, A674 (1964).  
<sup>5</sup>L. Willets and D. F. Gallaher, *Phys. Rev.* **147**, 13 (1966).  
<sup>6</sup>Francis J. Smith, *Proc. Phys. Soc. (London)* **84**, 889 (1964).  
<sup>7</sup>I. M. Cheshire, *J. Phys. B* **1**, 428 (1968).  
<sup>8</sup>L. T. Sin Fai Lam, *Proc. Phys. Soc. (London)* **92**, 67 (1967).  
<sup>9</sup>L. D. Landau and E. M. Lifshitz, *Mechanics* (Addison-Wesley, Reading, Mass., 1960), p. 56.  
<sup>10</sup>V. Dose, *Helv. Phys. Acta* **41**, 261 (1968).  
<sup>11</sup>W. Lichten, *Phys. Rev.* **131**, 229 (1963).  
<sup>12</sup>W. Lichten, *Phys. Rev.* **139**, A27 (1965).  
<sup>13</sup>V. Dose and V. Meyer, *Phys. Letters* **23**, 69 (1966).  
<sup>14</sup>I. A. Sellin, *Phys. Rev.* **136**, A1245 (1964).  
<sup>15</sup>D. H. Crandall, R. H. McKnight, D. H. Jaecks (unpublished).  
<sup>16</sup>P. Carr, *Vacuum* **14**, 37 (1964).  
<sup>17</sup>R. H. McKnight, D. H. Crandall, D. H. Jaecks, *Rev. Sci. Instr.* **41**, 1282 (1970).  
<sup>18</sup>B. L. Schram, A. J. H. Boerboom, W. Kleine, and J. Kistemaker, *Physica* **32**, 749 (1965).  
<sup>19</sup>D. H. Jaecks, B. Van Zyl, and R. Geballe, *Phys. Rev.* **137**, A340 (1965).  
<sup>20</sup>E. P. Andreev, V. A. Ankudinov, and S. V. Bobashev, *Zh. Eksperim. i Teor. Fiz.* **50**, 565 (1966) [*Sov. Phys.* **23**, 375 (1966)].  
<sup>21</sup>J. E. Bayfield, *Phys. Rev.* **182**, 115 (1969).

- <sup>22</sup>H. A. Bethe and E. E. Salpeter, *Quantum Mechanics of One and Two Electron Atoms* (Academic, New York, 1957), Secs. 67 and 63.  
<sup>23</sup>D. H. Jaecks, R. H. McKnight, and D. H. Crandall, in *Abstracts of VI International Conference on the Physics of Electronic and Atomic Collisions* (MIT, Cambridge, Mass., 1969), p. 862.  
<sup>24</sup>R. H. Hughes, C. A. Stigers, B. M. Doughty, and E. D. Stokes, *Phys. Rev. A* **1**, 1424 (1970).  
<sup>25</sup>W. L. Fite, W. E. Kauppila, and W. R. Ott, *Phys. Rev. Letters* **20**, 409 (1968).  
<sup>26</sup>W. R. Ott, W. E. Kauppila, and W. L. Fite, *Phys. Rev. A* **1**, 1089 (1970).  
<sup>27</sup>I. A. Sellin, J. A. Biggerstaff, and P. M. Griffin, *Phys. Rev. A* **2**, 423 (1970).  
<sup>28</sup>J. Macek (private communication).  
<sup>29</sup>D. H. Crandall, Ph.D. thesis (University of Nebraska, 1970) (unpublished).  
<sup>30</sup>L. I. Schiff, *Quantum Mechanics*, 3rd ed. (McGraw-Hill, New York, 1968), p. 155.  
<sup>31</sup>J. A. Smit, *Physica* **2**, 104 (1935).  
<sup>32</sup>T. A. Green, H. E. Stanley, and You-Chien Chian, *Helv. Phys. Acta* **28**, 109 (1965); also T. A. Green, *Phys. Rev.* **152**, 18 (1966).  
<sup>33</sup>R. K. Colegrave and D. B. L. Stephens, *J. Phys.* **B 1**, 856 (1968).  
<sup>34</sup>L. Pauling, *Chem. Rev.* **5**, 173 (1928); also L. Pauling and E. B. Wilson, *Introduction to Quantum Mechanics* (McGraw-Hill, New York, 1935), pp. 314–331.  
<sup>35</sup>H. H. Michels, *J. Chem. Phys.* **44**, 3834 (1966).  
<sup>36</sup>D. H. Jaecks, D. H. Crandall, and R. H. McKnight, *Phys. Rev. Letters* **25**, 491 (1970).  
<sup>37</sup>R. H. McKnight and D. H. Jaecks, following paper, *Phys. Rev. A* **4**, 2281 (1971).  
<sup>38</sup>C. E. Moore, *Atomic Energy Levels*, Natl. Bur. Std. Circ. No. 467 (U.S. GPO, Washington, D. C., 1949), Vol. 1.